

# MULTI-HARMONIC BUNCHER EXPERIMENT OVERVIEW FOR THE ISOLDE SUPERCONDUCTING RECOIL SEPARATOR PROJECT

I. Bustinduy\*, K. Altenmüller, I. de los Bueis, D. Fernandez-Cañoto, P. González, R. González, G. Harper, J. Martín, R. Miracoli, J. Muñoz, S. Varnasseri, A. Zugazaga  
ESS Bilbao, Zamudio, Spain

## Abstract

The ISOLDE Superconducting Recoil Separator (ISRS) at CERN is a rotatable high-resolution spectrometer able to separate reaction fragments induced by HIE-ISOLDE beams, from the lightest to the heaviest nuclear species, at collision energies up to 10 MeV/u. The injection of the ISOLDE beam into this ring requires a more compact bunch structure, so a Multi-Harmonic Buncher (MHB) device was designed for this task. The MHB will operate at a frequency of 10.128 MHz, which is a 10 % of the linac frequency, and would be installed before the RFQ. The MHB was designed as a two-electrode system, and the RF signal composed for the first four harmonics of the fundamental frequency, is fed into the electrodes. The system was first tested in the laboratory up to the nominal power conditions. Prior to delivery of MHB to its final location in ISOLDE, it will be tested with ion source beam at ESS-Bilbao with a  $\beta$  equal to 0.00328. In order to measure the functionality and characteristics of the produced bunches, a set of diagnostics were foreseen. To evaluate beam transmission a set of ACCTs and a Faraday Cup were employed, a Wien filter (WF) to measure energy, and a Fast Faraday Cup (FFC) for bunch length measurement. The preparation of the experiment along with the results are presented in this contribution.

## INTRODUCTION

The ISOLDE Superconducting Recoil Separator (ISRS) [1] requires a longer bunch spacing than that delivered by the HIE-ISOLDE linac. To meet this need, the ISRS programme at ESS-Bilbao is developing a multi-harmonic buncher (MHB) operating at 10.128 MHz, one tenth of the linac frequency, so that the beam can be rebunched while remaining synchronized with the downstream accelerator. The package delivered by ESS-Bilbao combines the buncher cavity, the RF generation and control chain, and a dedicated set of beam diagnostics. The MHB design evolved from early concepts [2] toward a wedge-electrode geometry optimized for the ISOLDE beam conditions [3]. On the RF side, the required sawtooth-like waveform is synthesized from the first four harmonics and stabilized with a digital low-level RF control system. The experimental line also includes ACCT current transformers, a Faraday cup, a Wien filter (WF), and a fast Faraday cup (FFC) for future bunch-length measurements [4]. To prepare beam commissioning, the ESS-Bilbao injector was configured to reproduce the reduced velocity required for the ISOLDE

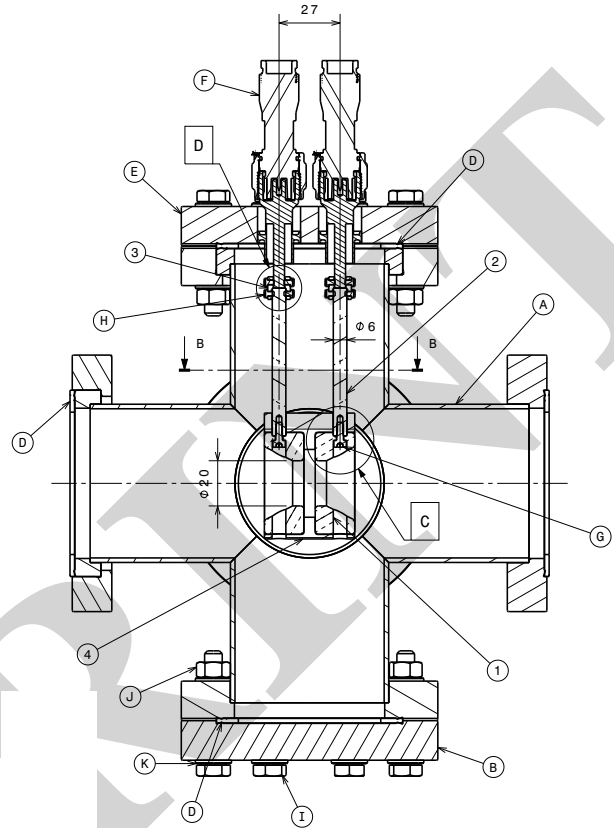


Figure 1: MHB Technical drawing: (1) MHB electrode, (2) Electrode support guide, (3) MHB electrode contact barrel, (4) MHB electrode spacer, (F) HN type male connector, (E) Forethought.

case,  $\beta = 0.00328$ . For this reason, in Bilbao, 10.094 keV  $H_2^+$  was selected as the commissioning species to adjust the parameters to the intended ISOLDE application.

## MHB MANUFACTURING

Due to the intended final location of the MHB in the ISOLDE linac, before the REX RFQ, a standard 4 way CF63 vessel has been chosen. One of the critical elements is the required feed-through for the electrodes. We have chosen a tailor made double CF63 HN connector based on the VA-COM W-HN50-GS-SE-CE-NI model. This model can work up to 7 GHz and up to 7 kV DC voltage. Among the many studied models, the version 4 (see Fig. 1) is the preferred solution due to its versatility. The maximum field at the required power is monitored by means of electromagnetic simulations to ensure Kilpatrick limit is not reached, currently this value is  $< 0.85$  MV/m (Kilpatrick 5.4 MV/m).

\* ibustinduy@essbilbao.org

Thermo-mechanical simulations show active cooling is not needed for the given heat load. To guarantee the required concentricity between electrodes, a Ketrion 1000 PEEK spacer and spacer barrels were considered. FEM simulations did not appreciate substantial effects from these elements in the electromagnetic fields.

## RF SYSTEM

The RF chain is composed of a low-level generation and control stage, a driver amplifier, a high-power amplifier and a balanced coupling stage. The driver stage is based on the LZ-Y-22+ RF amplifier, which provides up to 30 W over a wide operating bandwidth of 0.1 MHz to 200 MHz, therefore covering the complete frequency range required by the MHB harmonics. This unit includes protection against over-temperature conditions and tolerance to short- and open-load situations, and is operated from a 24 V/5.5 A DC power supply. The driver feeds the RFE-24M30M1K7X+ solid-state high-power amplifier module, which is able to amplify CW and pulsed RF signals to power levels above 1700 W. This module includes temperature-compensated gate biasing, temperature and current monitoring, and an external TTL emergency shutdown input, which can be used to protect the system in case of excessive reflected or dissipated power. Since the MHB electrodes constitute a balanced load while the RF amplifier output is an unbalanced 50  $\Omega$  coaxial line, a 9:1 balun is inserted between the amplifier and the cavity. This balun transforms the 50  $\Omega$  unbalanced input into an approximately 450  $\Omega$  balanced output, matching the MHB electrode system and multiplying the voltage by a factor close to three under ideal lossless conditions.

## COMMISSIONING

In order to adjust precisely the specimen energy required by the experiment, we had to adjust iteratively the extraction voltage setting in the ion source high voltage platform, while optimizing the optical transmission conditions in the LEBT solenoids and conducted sequentially to minimize perturbations on the plasma behaviour variations.

The commissioning campaign started with beam transport studies. In the first part, the team optimized the LEBT solenoids to enhance  $H_2^+$  transmission and benchmarked the results against RF-Track [5] simulations, obtaining good agreement in the observed transmission peaks. One of the major identified experiment limitation was a significant high voltage droop during the pulse length, which translated into a measurable kinetic variation along the pulse. As a consequence, our model had to focus on a particular narrow region of interest next to  $1 \times 10^3$   $\mu s$  to keep certain consistency.

The main purpose of the WF is to calibrate the beam energy and species composition. Since the magnetic field of the WF was slightly different from the magnetic model, the relation between estimated kinetic energy  $\omega_i$  of each specimen with voltage difference between WF electrodes was inferred empirically. This allowed us to express the collected data as a function of estimated kinetic energy  $\omega_i$

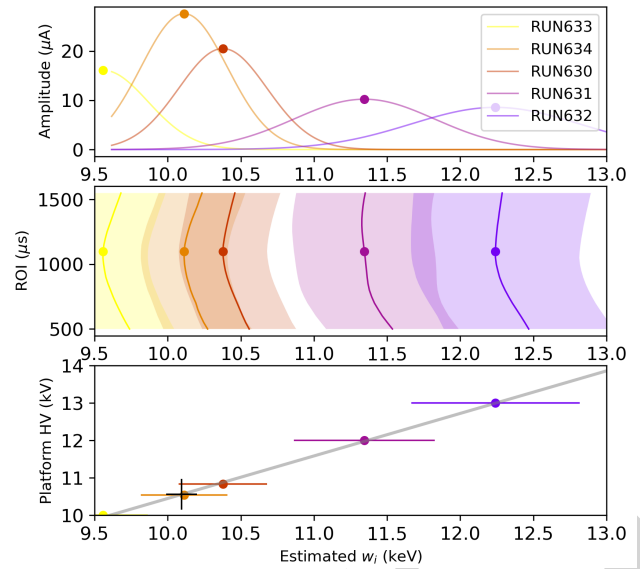


Figure 2: **Upper-frame:** beam current gaussian fit profile shapes. **Middle-frame:** center and sigma estimation for each Region of interest. **Bottom frame:** Wien filter center and sigma for each extraction voltage setting.

(see Fig. 2). This Fig. represents the collected data fitted to  $n$  Gaussian for each region of interest (ROI) in units of time ( $\mu s$ ). And therefore, estimate the required platform voltage setting to get the desired  $\omega_i = 10.094$  keV that results in the same  $\beta$  as required by the ISOLDE experiment. According to this approach, the required voltage would be 10.55 kV, with a  $R^2$  coefficient of determination equal to 0.9988.

## Optimization

The ESS-Bilbao injector was originally conceived for 45 keV  $H^+$  beams. So, in order to run this experiment for ISOLDE, LEBT solenoids were required to be tuned to enhance  $H_2^+$  transmission. Classical optimization approaches were first evaluated, followed by Bayesian optimization and population-based methods. In dedicated steering campaigns, Gaussian process and random-forest-based Bayesian minimization [6] rapidly improved transmission, while more advanced multi-objective optimization techniques [7] allowed the team to optimize beam current and pulse flatness simultaneously.

The objective, as described in Fig. 3 is to seek the best steerer solenoid configuration that provides both maximum current at the second Faraday cup (FC2), and the second

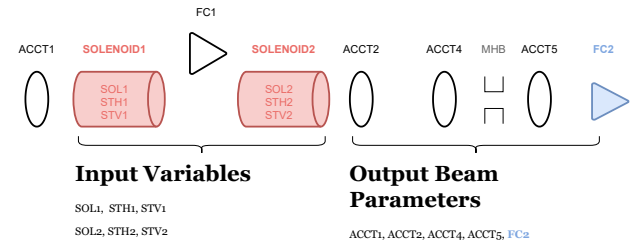


Figure 3: Schematic view of the input variables and the output beam parameters.

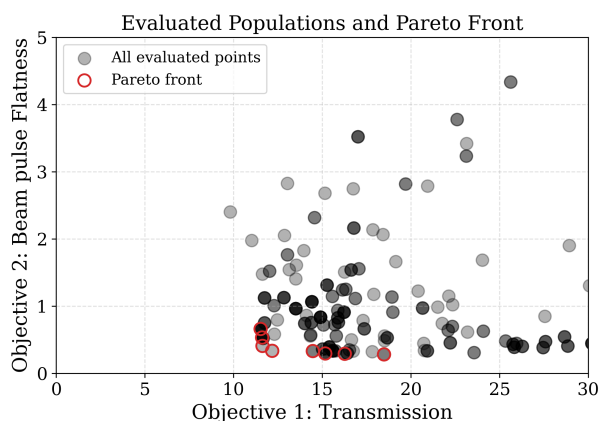


Figure 4: Evaluated population and Pareto front for the four steerer multi-objective optimization problem. Each point represents a certain combination of four steerers.

objective is to have a homogenous beam pulse shape. Several derivative-free optimization strategies were investigated for noisy linac tuning. Particle Swarm Optimization (PSO) offers a simple population-based search and can rapidly identify promising regions of the parameter space. However, in noisy experimental conditions its velocity update can be strongly affected by outlier measurements, leading to premature convergence or stagnation. NSGA-II, on the other hand, offered a clear advantage when the linac tuning problem is treated as a genuine multi-objective optimization problem. As shown in Fig. 4, rather than combining transmission, pulse flatness, stability, or other beam-quality indicators into a single merit function, NSGA-II evolves a population of candidate machine settings toward a Pareto front. This provides a set of trade-off solutions from which the operator can select the most appropriate working point according to experimental priorities or hardware constraints. In this sense, GP-based Bayesian optimization was the most effective approach for efficient scalar optimization, whereas NSGA-II was more suitable for preserving the multi-objective nature of the problem.

## CONCLUSIONS AND FUTURE WORK

The results presented in this work demonstrate the advanced stage of the ISRS-SPAIN MHB project. They show that AI-assisted and numerical optimization approaches can improve beam transport performance, reduce commissioning effort, and provide a solid basis for intelligent and adaptive accelerator operation. In particular, the optimization techniques applied to the LEPT steering system increased the beam transmission by more than 30%, while requiring only a limited number of machine evaluations. In addition, the combined use of beam dynamics simulations, solenoid scans, and Wien-filter measurements provided a consistent framework for identifying the relevant hydrogen species, benchmarking the transport model, and characterizing the beam energy.

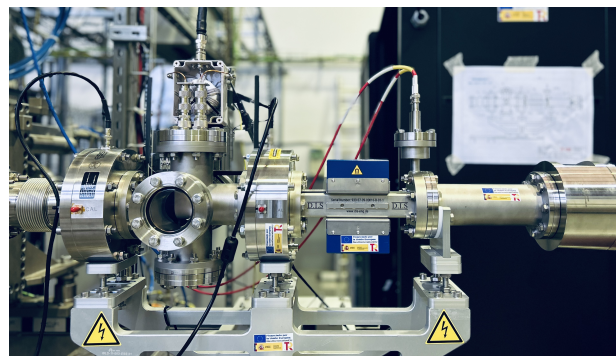


Figure 5: MHB experiment configuration assembly. From left to right: ACCT, MHB, ACCT, WF, FFC

In the coming months, the RF amplifier will be connected directly to the MHB cavity, and the bunched beam will be characterized with the Fast Faraday Cup installed at the end of the line, as shown in Fig. 5. By combining Wien-filter energy selection with nanosecond-resolved current measurements, we aim to reconstruct the longitudinal phase space of the beam and complete the first full validation of the MHB concept under realistic operating conditions.

## ACKNOWLEDGMENTS

This work was funded by Spanish MCIN, Recovery and Resilience Funds, and European Union "NextGenerationEU".

## REFERENCES

- [1] I. Martel *et al.*, "An innovative superconducting recoil separator for hie-isolde", *Nucl. Instrum. Methods Phys. Res. B*, vol. 541, pp. 176–179, 2023. [doi:10.1016/j.nimb.2023.05.052](https://doi.org/10.1016/j.nimb.2023.05.052)
- [2] M. A. Fraser, "Beam dynamics studies of a multi-harmonic buncher for 10 MHz post-accelerated RIBs at HIE-ISOLDE", CERN, Geneva, Switzerland, Project Note HIE-ISOLDE-PROJECT-Note-0035, Nov. 2014. <https://cds.cern.ch/record/1972434>
- [3] J. L. Muñoz *et al.*, "Multi-Harmonic Buncher (MHB) studies for protons and ions in ESS-Bilbao", in *Proc. LINAC'22*, Liverpool, UK, pp. 334–336, Oct. 2022. [doi:10.18429/JACoW-LINAC2022-TUP0J002](https://doi.org/10.18429/JACoW-LINAC2022-TUP0J002)
- [4] S. Varnasseri, I. Bustinduy, P. J. González, R. Miracoli, and J. L. Muñoz, "Stripline Design of a Fast Faraday Cup for the Bunch Length Measurement at ISOLDE-ISRS", in *Proc. HB'23*, Geneva, Switzerland, pp. 426–428, Mar. 2024. [doi:10.18429/JACoW-HB2023-THAFP10](https://doi.org/10.18429/JACoW-HB2023-THAFP10)
- [5] A. Latina, "RF-Track Reference Manual", Jun. 2020. [doi:10.5281/zenodo.4580369](https://doi.org/10.5281/zenodo.4580369)
- [6] R. Roussel *et al.*, "Bayesian optimization algorithms for accelerator physics", *Phys. Rev. Accel. Beams*, vol. 27, no. 8, p. 084801, Aug. 2024. [doi:10.1103/PhysRevAccelBeams.27.084801](https://doi.org/10.1103/PhysRevAccelBeams.27.084801)
- [7] K. Deb, A. Pratap, S. Agarwal, and T. Meyarivan, "A fast and elitist multiobjective genetic algorithm: NSGA-II", *IEEE Trans. Evol. Comput.*, vol. 6, no. 2, pp. 182–197, 2002. [doi:10.1109/4235.996017](https://doi.org/10.1109/4235.996017)